TDR 2006
Purdue University

Role of Soil Density and Solute Concentration on Water Content Detection in Soil Using TDR

Abdel-Mohsen O. Mohamed and Nuha Abbas

Ref.: Mohamed, Abdel-Mohsen O. and Abbas, Nuha, "Role of Soil Density and Solute Concentration on Water Content Detection in Soil Using TDR", Proc. TDR 2006, Purdue University, West Lafayette, USA, Sept. 2006, Paper ID 8, 13 p., https://engineering.purdue.edu/TDR/Papers

Role of Soil Density and Solute Concentration on Water Content Detection in Soil Using TDR

Abdel-Mohsen O. Mohamed[1] and Nuha Abbas[2]

[1] Advisor to the Assistant Provost for Research and Professor of Geotechnical and Geoenvironmental Engineering, Department of Civil and Environmental Engineering, U.A.E. University, Al-Ain, P.O. Box: 17555, UAE, e-mail: Mohamed.a@uaeu.ac.ae

[2] Research Assistant, Department of Civil and Environmental Engineering, U.A.E. University, Al-Ain, P.O. Box: 17555, U.A.E.

Abstract

This study seeks to evaluate the role of soil density and solute concentration on water content detection using a TDR probe system and eigendecomposition method. As a demonstration, specimens with variable amounts of bentonite (0 to 6% by wt.), water contents (0 to 20% by wt.) and concentrations (0ppm and 1200ppm) were compacted at known densities and tested using TDR probe. For each experiment, reflected signals were captured by an oscilloscope and their characteristics were identified using eigendecomposition method. Autoregressive modeling and singular value decomposition methods were utilized for calculating the eigenvalues. The most significant eigenvalues were then identified based on their power. Experimental results indicated that the presented system is sensitive to soil density, solute concentration, moisture and clay contents in the tested specimens. Multivariate statistical analysis was then performed and the regression analysis resulted in a system of nonlinear equations that best described the system. Actual and predicted results are in agreement, indicating a good performance and versatility of the developed system for wide range of water and clay contents in the tested samples.

Key Words: eigendecomposition, autoregressive modeling, singular value decomposition, eigenvalues, eigenvectors, multivariate statistical analysis, nonlinear analysis, bentonite, sodium chloride.

Introduction

Time Domain Relectrometry (TDR) detection operates by analyzing the characteristics of a fast rising electric potential signal as it reflects at a probing end of a transmission structure (coaxial cable for example) immersed in a sample under investigation. The characteristics of the reflecting signals are highly influenced by the electrical properties of the sample, which are dependent on the physico-chemical properties of the pore fluid, soil structure and minerals, initial placing conditions, and temperature.

Soil water content, from TDR measurements, is generally calculated using the widely known formula developed by Topp [1] who found a solitary polynomial function that described the relationship between volumetric water content and apparent dielectric constant for mineral soils, which is given as

$$\theta = -5.3\cdot 10^{-2} + 2.92\cdot 10^{-2}\cdot \varepsilon_b - 5.5\cdot 10^{-4}\cdot {\varepsilon_b}^2 + 4.3\cdot 10^{-6}\cdot {\varepsilon_b}^3 \qquad (1)$$

where θ is the volumetric soil water content, ε_b is the apparent permittivity of the soil. Topp's equation is a pure empirical equation derived from fitting curves of experiment results on a wide range of soils with different moisture contents. However, from the analysis of soil bulk dielectric, we know that volumetric fraction of water is not the only factor contributing to the bulk dielectric constant. Although Topp's equation is regarded as a universal calibration function, immediate concerns should be toward the validity of such equation for predicting moisture content of soils with different textures, surface areas, organic contents, density, and salinity.

In the applications of using TDR system in sandy and loamy soils with little or no electrical conductivity, many researchers reported high accuracy of using Topp's equation. Some of the reported tests are for: (1) fine sand with volumetric water content ranging from 0.05 to 0.35 [2]; (2) sandy loam [3]; (3) sandy and loamy soils with air dry and saturated cases [1]; and (4) sand and silty soils [4].

However, glass beads, clay and high organic content soils showed apparent deviation from this empirical function. The error could be as high as 0.03 in predicted volumetric water content. Some reported tests are: (1) for glass beads with variable diameters ranging from 30 to 450 μm, it was found that the volumetric water content was overestimated [1]; (2) for clay soils, it was found that the volumetric water content was underestimated [1]; (3) for high organic tropical soils with low density of 0.7 Mg/m^3 and variable volumetric water contents ranging from 0.0 to 0.5, the predicted water content was underestimated [5]; (4) soils having high clay and organic contents deviate sharply from Topp's empirical functions.

It is known that soil fractions safeguard our natural waters by attenuating pollutant migration. Soils can adsorb pollutants, buffer pH, aid in the precipitation of pollutants, and host biological activity that may transform or degrade pollutants. Specifically, attenuation occurs by mechanisms such as adsorption, complexation, precipitation, filtration, and biological degradation. The non-living components that may contribute to the retention of pollutants can be either organic or inorganic. The organic fractions are composed of unaltered organic matter such as plant roots, transformed organic matter such as amorphous humic substances and decayed materials [6, 7]. The organic fraction is composed of both crystalline and amorphous materials. The crystalline portion is composed of primary and secondary minerals with primary minerals forming a major portion of sand and silt size particles and a minor part of the clay size fraction. The clay size fraction is composed predominately of layer silicates that are generally described as clay minerals. Mixed in and perhaps coating the soil particles are carbonates and amorphous materials such as oxides, hydroxides, and oxyhydroxides. These components along with the layer lattice clay mineral particles and organic fraction make up the most active components of a soil and control its engineering properties. The question is how much control does each component exercise on the resultant dielectric properties that contribute to the measured response of an electric signal?

Therefore, the overall objectives of the study are: (1) evaluate the contribution of each component in the soil mix design on the response electric signals; (2) utilize the newly developed TDR technique for detecting pollutants in subsurface environment as well as the novel data analysis technique; and (3) develop a method for relating the properties of the response signal to the component mix design.

In this part of the investigation we will be looking to evaluate the effect of soil density, solute concentration, clay fraction, and water content on the response electric signals and analyze the reflected TDR signals using eigendecomposition method.

Theory

Detection by TDR

In brief, a monitoring probe, machined from a conducting rod (reference), is connected to a pulse generator and to an oscilloscope via a transmission line (coaxial cables). The oscilloscope is used to acquire the system response through a measurement point on the transmission line. During measurement, an electrical pulse with a fast rising edge is generated periodically by the pulse generator and launched toward the probe. The pulse signal propagating toward the probe appears on the oscilloscope as it passes the measurement point located at a known distance from the generator on the transmission line. As the pulse reaches the probe end, it reflects back on the transmission line with pulse characteristics dependent on the properties of the media surrounding the probe. The reflected pulse signal propagates back toward the generator and, thus, appears on the oscilloscope after a delay time with respect to the time of appearance of the original pulse. The delay time is representative of the distance traveled by the pulse from the measurement point to the probe end and back to the measurement point, as well as the electrical characteristics of the media surrounding the probe. Equally important is the magnitude of the reflected signal, which is also highly dependent on the electrical properties of the composition of the surrounding media.

Captured signals can further be analyzed by different methods such as Fourier spectral analysis [8-10], power spectral analysis [8, 9], and eigendecomposition [11-13]. In this study, eigendecomposition has been utilized because of its ability to isolate secondary signal components containing little power. Such secondary components may not be visible in Fourier spectra.

Eigendecomposition

In eigendecomposition analysis, an orthogonal set of expansion vectors are extracted to indicate dominant variablities in a collection of data points. The coordinates of the points along each vector will be an *eigenvector*, and the length of the projection will be an *eigenvalue* [13, 14]. Processing of eigenmodes (eigenvectors and eigenvalues/ singular values) of a data series is an important tool in signal analysis [15]. Unlike Fourier decomposition, which partitions signals based on harmonic frequency using parametric sines and cosines, an eigendecomposition partitions signals by their strength using adaptive non-parametric basis functions. Signal components can thus be separated by differences in power. The first eigenmode captures the greatest measures of the variance in the data; the least eigenmode usually captures only the least significant noise oscillations. It does not matter if the component captured is sinusoidal, a square wave, a sawtooth, or anharmonic pattern. Further, the signal may be slowly varying low frequency anharmonic oscillation, or a high frequency sinusoid. The strength of eigendecomposition is the isolation of secondary signal components containing little power. Such secondary components may not be visible in Fourier spectra because of spectral leakage and resolution reasons.

In the eigendecomposition procedure, the main task is to set a sorted eigenvalue threshold whereby the noise that is present in the signal can be removed. All of the eigenmodes are used in the reconstruction of the signal. The principal components of the signal will be captured in the initial eigenmodes while the noise is broken into low power elements. An eigendecomposition can be achieved in any number of ways [8, 9, 11, 15]. The first step is always the creation of a matrix that uses lagged copies of subsets of the data series. This can be a straightforward data or trajectory matrix, such as the forward prediction (Fwd), backward prediction (Bwd), or forward-backward (FB) prediction matrices used in autoregressive (AR) modeling. These data matrices are usually rectangular, and singular value decomposition (SVD) is used to extract the eigenvectors and singular values. Detailed description of the method of analysis can be found in Mohamed et al. [13].

***Autoregressive modeling* (AR)**

In an AR modeling, a value at time *t* is based upon a linear combination of prior values (Fwd prediction), upon a combination of subsequent values (Bwd prediction), or both (FB prediction). The linear models give rise to rapid robust computations [8, 9]. To preserve the degrees of freedom for statistical tests and to furnish a common reference for all AR algorithms, the AR model is represented as follows:

$$y_k = \sum_{j=1}^{M} a_j x_{k+j} \qquad k = M \cdots\cdots 1 \tag{2}$$

$$y_k = \sum_{j=1}^{M} a_j x_{k-j} \qquad k = M+1 \cdots\cdots N \tag{3}$$

In these equations (2 and 3) x is the data series of length N, and a is the autoregressive parameter array of order M. The model is defined as reverse prediction for the first M values, and forward prediction for the remaining N-M values.

The AR coefficients can be computed in a variety of ways. The coefficients can be computed from autocorrelation estimates, from partial autocorrelation (reflection) coefficients, and from least squares matrix procedures. Further, an AR model using the autocorrelation method will depend on the truncation threshold (maximum lag) used to compute the correlations. The partial autocorrelation method will depend on specific definition for the reflection coefficient. The least squares methods will also yield results that are a function of how data are treated at the bounds (matrix size) as well as whether the data matrix or normal equations are fitted.

A basic AR model fit does not offer effective signal noise partitioning [8, 9]. Even if pure sinusoids are embedded in a modest level of noise, it may require an order well beyond twice the signal component count to successfully capture and spectrally render the sinusoids. In other words, if the model order is too low, only a portion of the deterministic signal is captured. The remainder is treated as part of the white noise (Gaussian distributed). Spectral components are thus missed. On the other hand, if a model order is too high, the full deterministic signal is captured but some measure of the noise is also modeled. There are three ways to manage this limitation. First, the noise can be filtered or removed prior to analysis. Second, an optimum AR order can be selected that captures all the deterministic signal elements and includes as little noise as possible. The third option consists of an in situ noise removal within the least squares procedures that generate the coefficients, which can be accomplished using singular value decomposition (SVD) in any of the least squares AR models [8, 9].

***Singular value decomposition* (SVD)**

This technique is generally used when Gaussian elimination and Lower and Upper (LU) decomposition fail to give satisfactory results. SVD is also the method of choice for solving most linear least-squares problems. SVD methods are based on the theory of linear algebra as discussed by Press et al. [11].

The decomposition of any matrix A_{ij} can be expressed as a sum of outer products of columns of U and rows of V^T, with the "weighting factors" being the singular values w_j.

$$A_{ij} = \sum_{k=1}^{N} w_k U_{ik} V_{jk} \tag{4}$$

where U and V are orthogonal matrices in the sense that their columns are orthonormal.

***Solution by use of singular value decomposition* (*SVD*)**

Consider the set of simultaneous Eqs. 2 and 3 and rewrite them in a general form as:

$$y = A \bullet x \tag{5}$$

where y is the predicted vector, A is the autoregressive parameter array and x is a vector containing the data series.

The least-squares solution vector x is given by:

$$x = V \bullet \left[diag(1/w_j) \right] \bullet (U^T \bullet y) \tag{6}$$

To obtain a solution, one finds x that minimizes

$$\chi^2 = \left| A \bullet x - y \right|^2 \tag{7}$$

Then, the solution of Eq. 7, can be written as:

$$x = \sum_{i=1}^{M} \left(\frac{U_i \bullet y}{w_i} \right) V_i \tag{8}$$

The variance in the estimate of a parameter x_j is given by:

$$\sigma^2(x_j) = \sum_{i-1}^{M} \frac{1}{w_i^2} \left(V_i \right)_j^2 = \sum_{i=1}^{M} \left(\frac{V_{ji}}{w_i} \right)^2 \tag{9}$$

and the covariance is given by:

$$Cov(x_j, x_k) = \sum_{i=1}^{M} \left(\frac{V_{ij} V_{ki}}{w_i^2} \right) \tag{10}$$

Experimentation

TDR System Setup

The schematic diagram shown in Figure 1 illustrates the arrangement of the measurement system. The pulse generator is connected via a transmission line (coaxial cable) to the output (OUT) port of the directional coupler and the probe is connected via another transmission line to the input (IN) port of the directional coupler. An oscilloscope is connected to the coupled (CPL) port of the directional coupler via a third transmission line. In this arrangement, the output signal from the pulse generator is transmitted only to the probe while the reflected signal is coupled to the oscilloscope for recording. Since, incident pulses do not appear on the oscilloscope, signal separations into incident and reflected become an easy task for further data analysis.

The probe consists of a signal line and a ground conductor and terminates at the coaxial cable end at the sample side.The probe structure was fabricated using a 90 *mm* long aluminum rod with a diameter of 10 *mm* and a ground disc. The probe length was determined by considering the probe as a monopole structure, which has an infinite ground plane as reeported by Said et al., [16] and Mohamed et al., [10]. If such a plane is folded in cylindrical coordinate system, then a coaxial transmission line is obtained. In the designed probe, the ground plate (the circular disk) has a relatively small extent. To extend the ground plane of the probe, while maintaining the compactness of the probe design, two conducting rods have been attached to the ground plane. Adding the two conducting rods to the ground plane does not alter the probe structure to a three-wire transmission line. In fact adding more conducting rods to the ground plane will enhance the coupling between the monopole and the ground plane, but would on the other hand limit the extent of the area being probed and add difficulty to inserting the probe in solid media, such as sand. The attached rods had a diameter measuring 2.5 *mm* and were placed at a distance of 17.5 *mm*, center-to-center, from the monitoring probe.

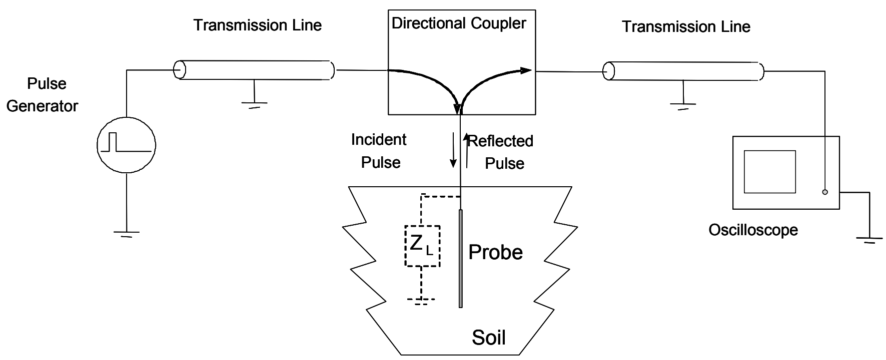

Figure 1: Schematic drawing of the used TDR system arrangement showing the pulse generator, probe, oscilloscope, and the directional coupler which isolates the reflected signal for simplified signal processing.

The used coaxial cables had a line capacitance of 101 pF/m and an impedance of 50 Ω for connecting the pulse generator, the measuring probe and the oscilloscope. A 3.6 m long cable was used to allow enough time delay for the reflected pulse to appear on the oscilloscope screen. The pulse repetition rate was 8.3 MHz, amplitude of 1V, and rise and fall time was about 3 nano-seconds. Figure 2 shows a plot of the applied pulse as captured by the oscilloscope with an illustration of the different pulse parameters. It should be pointed out that each pulse is composed of infinite number of sinusoidal harmonic frequencies of the fundamental frequency 8.3 MHz. These harmonics are the Fourier components of the pulse.

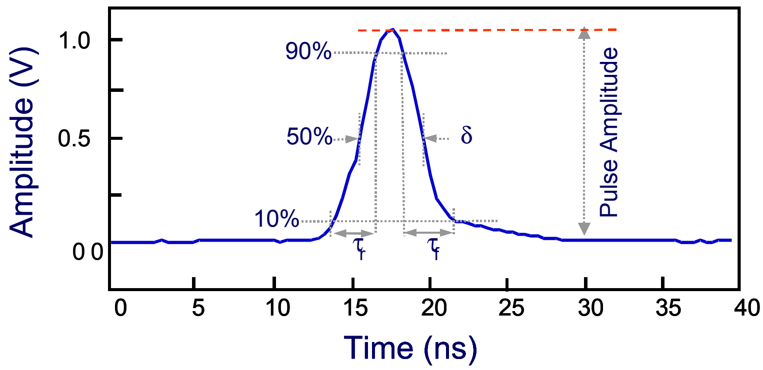

Figure 2: A plot of the generated pulse used in the measuring system as captured on the oscilloscope.

Materials

The soil material used in this investigation is sand dune obtained from Al Ain district, UAE, mixed with different amounts of bentonite obtained from Abu Dhabi National Oil Company (ADNOC), Abu Dhabi, UAE. The selected testing procedures were carried out following procedures described by ASTM standards [19].

The experimental results indicated that the sand dunes had variable diameters ranging from 0.1 to 1 mm, specific gravity of 2.53, maximum dry density of 1.53 Mg/m^3, and optimum moisture content of 10%. The compaction characteristics of the mixed soil samples are shown in Figures 3 and 4. It can be seen that as the bentonite fraction increases the maximum dry density increases due to the increase of bentonite coatings to the sand grains and decreasing the voids ratio. At low added bentonite fraction (0- 4%) the optimum water content is decreased. Such behaviour is well known for ganular soils because of the "bulking phenomenon" and it seems that the added bentonite percent was not enogh to change such behaviour. Beyond the bentonite fraction of 4%, the optimum water content increases as expected.

Methods

Sample Preparation: Various sets of samples were prepared to study the system response to moisture and bentonite fraction contents. The bentonite fraction varied from 0% to 6% by weight with increments of 3% while the moisture content varied from 0 to 20% by weight in increments of 4%. Water with varying concentration of salt between 0 ppm and 1200ppm was used. The specimens were compacted in a known densities calculated from the equation in fig.4. Soil material was then placed in a testing column having 58 mm in diameter and 80 mm in length at a the maximum dry density calculated from Figure 3. Soil material was then placed in a testing column having 60 mm in diameter and 120 mm in length at a constant dry density of 1.62 Mg/m^3. It is worth noting that this low density was chosen because of the difficulties we have encountered during probe installation. It is understandable because of the high swelling capacity of bentonite, which made it difficult to drive the probe into the soil. For probe installation, a hole with a diameter slightly smaller less than that of the probe size was drilled through the compacted specimen and the testing probe was pushed through the compacted soil material. Then, the probe was connected to the oscilloscope as shown in Figure 1.

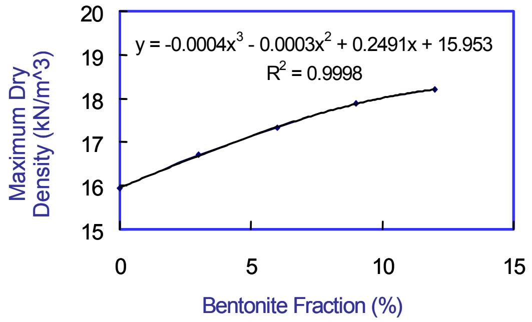

Figure 3: Maximum dry density variations with percent bentonite fraction in the sample

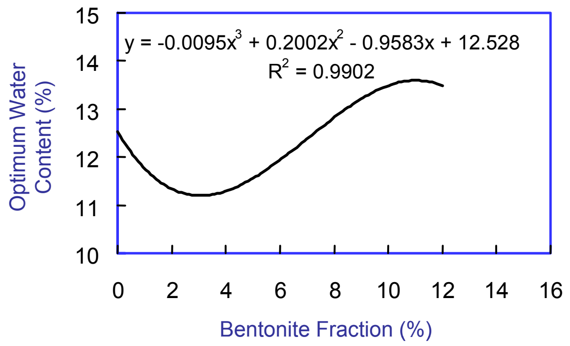

Figure 4: Optimum water content variations with percent bentonite fraction in the sample

Measurements*:* The setup shown in Figure 1 was adjusted, so that the oscilloscope could take 32 readings at a time and calculate the average. Special computer software (FlukeView^{TM}) was used to acquire the data measured for each test. Reflected signals were captured and recorded for each variation of moisture content and/or bentonite fraction.

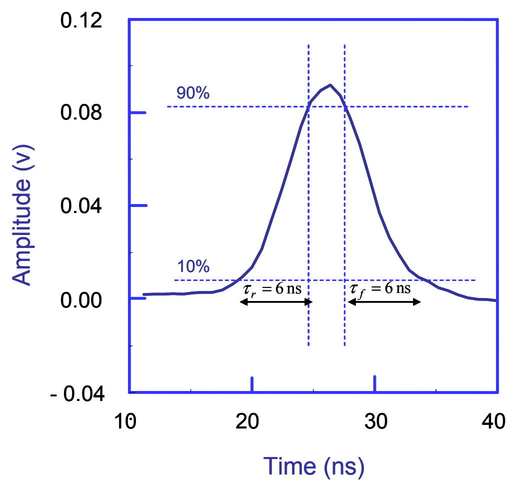

Figure 5: TDR reflected signal as captured on the oscilloscope, while the probe is held in air

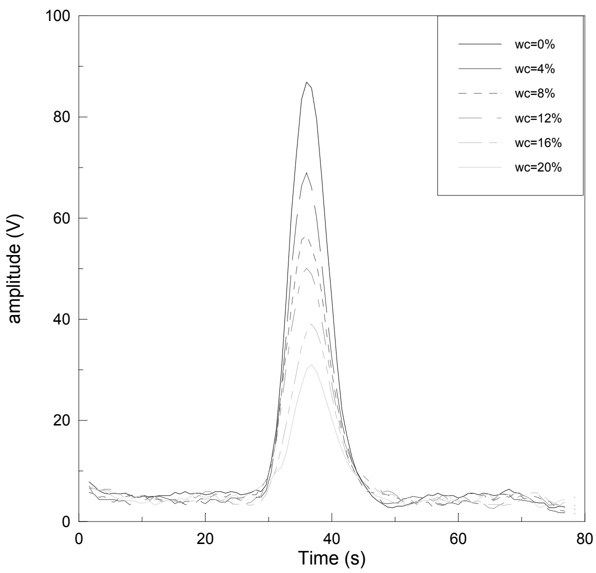

Figure 6: TDR reflected signal as captured on the oscilloscope for various water content of 200ppm salt concentration and 3% clay fraction.

Results and Discussion

Time Domain Results

Figure 5 shows the captured waveform for the probe held in air while Figure 6 shows the captured waveforms for soil mixed with water of 200ppm salt concentration at various water contents by weight and 3% bentonite fraction. The results indicate that as the moisture content increases, signal peak broadening as well as the signal width at 50% of its peak value increases. Also, as the moisture content increases, signal amplitude decreases and time delay increases. Normalizing the results shown in Figure 6 with respect to that shown in Figure 5, one can easily observe that as the moisture content increases, the relative signal amplitude decreases. This could be attributed to increase of medium capacitance and decrease of its resistance [17, 18].

Similar results captured with different values of salt concentration varying between zero and 1200ppm with increments of 200ppm (Figure 7). Figure 9 shows the effect of density on the signal captured of sample with 800ppm concentration and 6% clay content. The results in Figure 8 clearly indicate that as the density increases, signal width at 50% of its peak decreases. Furthermore, as density increases, reflected signal amplitude decreases and the time delay increases. In addition, as the density increases, the relative amplitude also decreases. This is so because as the density increases the soil medium dielectric constant and capacitance increases and its resistance decreased. These results are consistent with diffuse ion theory in which as dielectric constant increases soil water potential increases and medium capacitance increases [7]. To further analyze the preceding time domain experimental data, one uses the eigendecomposition technique that described above.

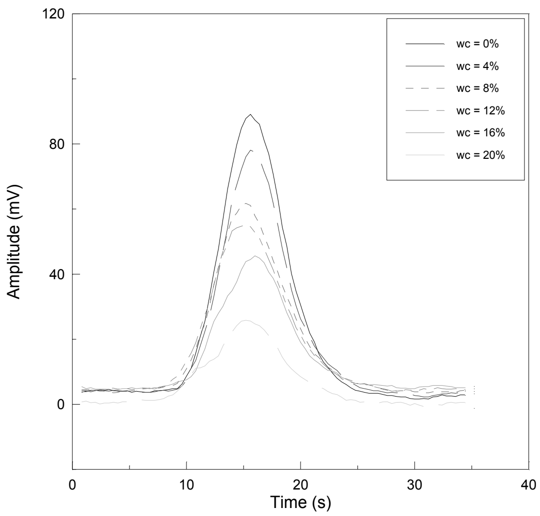

Figure 7: TDR reflected signal as captured on the oscilloscope for various water content of 800ppm salt concentration and 3% clay fraction.

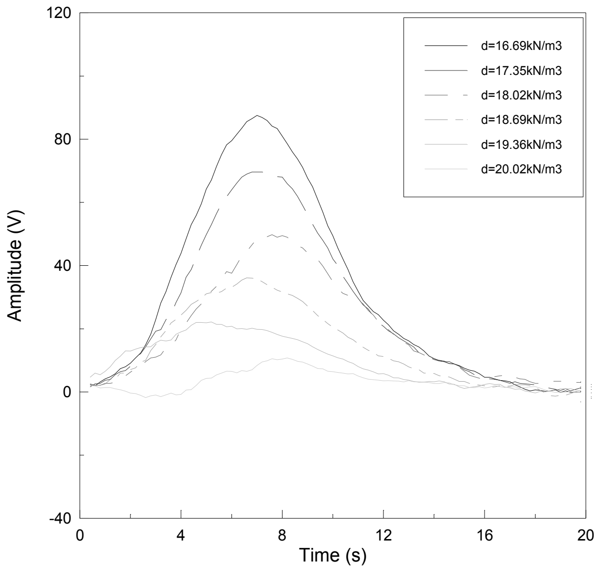

Figure 8: TDR reflected signal as captured on the oscilloscope for various water content of 600ppm salt concentration and 6% clay fraction.

Eigendecomposition Analysis

The eigendecomposition technique was utilized to analyze the experimental results for soils tested with various water contents and sample wet densities. Typical results for the calculated eigenvalues are shown in Figures 9 and 10 for bentonite fractions of 6 and 3%, respectively. These figures show the variations of the calculated eigenvalues (E_1 to E_5) with water and bentonite fractions and density respectively.

The results indicate that there are distinct variations at the first and second eigenvalues that represent the largest variations of the data as well the maximum power in the signal. For the same order of the eigenvalue and bentonite fraction, as water content (or density) increases the magnitude of the eigenvalues decreased (Figures 9 and 10). In addition, results shown in Figures 9 and 10 indicate that the variations of E_1 and E_2 are noticeable while E_3 to E_5 are not.

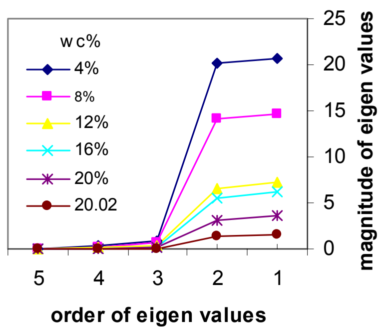

Figure 9: Variations of first five extracted eigenvalues as a function of water contents for soil samples with bentonite fraction of 6% and 600ppm salt concentration.

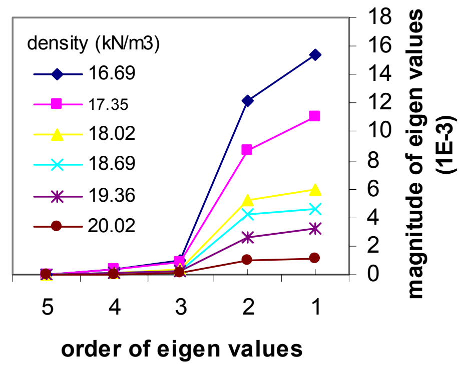

Figure 10: Variations of first five extracted eigenvalues as a function of density of soil samples with bentonite fraction of 3%and 800ppm salt concentration.

Determination of Water Content and density

The results recorded from TDR and the first four eignvalues obtained from eigendecomposition were analyzed using MINITAB to obtain relationships between the first four orders of eignvalues and water content and density of soil. Figure 11a shows the contour plot of the first eigenvalue, water content and density.

The following equations represent the nonlinear regression of the results:

$$\begin{aligned} \boldsymbol{W_c} = {} & 18.8 - 4.48\,\boldsymbol{E_1} + 2.50\,\boldsymbol{E_2} + 12.5\,\boldsymbol{E_3} + 4.6\,\boldsymbol{E_4} + 5.00\,\boldsymbol{E_1}^2 + 4.08\,\boldsymbol{E_2}^2 + 110\,\boldsymbol{E_3}^2 - 161\,\boldsymbol{E_4}^2 \\ & - 8.85\,\boldsymbol{E_1E_2} - 52.1\,\boldsymbol{E_1E_3} + 45.3\,\boldsymbol{E_1E_4} + 39.7\,\boldsymbol{E_2E_3} - 32.2\,\boldsymbol{E_2E_4} - 35\,\boldsymbol{E_3E_4} \end{aligned} \tag{11}$$

where E_1, E_2, E_3 and E_4 are the first four eignvalue of the reflected signal; W_C is the water content as a percent. The squared residuals of the fitting equation are 73.5%. That means the fitted regression model explains about 73.5% of the observed variations in amplitude [R^2 = 73.5%; R^2 (adjusted) = 69.1%]. The observed significance levels (p-values) of the T-test are all ≤ 0.9. Furthermore, the analysis of variance (ANOVA) F-test found to be 16.85, with 14 and 85 degrees of freedom, which indicates that the regression model is highly significant overall (the corresponding p-value is less than 0.0001). The predicted representations of the variations of water content $\boldsymbol{W_C}$ are shown in Figure 11b.

Similarly, the following nonlinear equation is obtained for E_2:

$$\gamma = 20.4 - 0.801\, \boldsymbol{E_1} + 0.404\, \boldsymbol{E_2} + 0.12\, \boldsymbol{E_3} + 3.39\, \boldsymbol{E_4} + 0.476\, \boldsymbol{E_1}^2 + 0.338\, \boldsymbol{E_2}^2 + 33.1\, \boldsymbol{E_3}^2 + 42.6\, \boldsymbol{E_4}^2 - 0.791\, \boldsymbol{E_1 E_2} - 8.46\, \boldsymbol{E_1 E_3} + 10.9\, \boldsymbol{E_1 E_4} + 7.28\, \boldsymbol{E_2 E_3} - 9.57\, \boldsymbol{E_2 E_4} - 77.9\, \boldsymbol{E_3 E_4} \quad (12)$$

where $\boldsymbol{\gamma}$ is the wet density of soil (kN/m^3). The observed significance level (p-values) of the T- test are all ≤ 0.97. Furthermore, the ANOVA F-test is found to be 47.12, with 14 and 85 degrees of freedom, which indicates that the regression model is highly significant overall (the corresponding p-value is less than 0.0001). In fact the fitted regression explains about 88.6% of the observed variations [R^2 = 88.6%; R^2 (adjusted) = 86.7%].

Therefore, during field operation reflected TDR signals will be analyzed using eigendecomposition and the first two eigenvalues will be used, in association with Eqs. 11 and 12, to predict the water content and clay fraction in the tested samples.

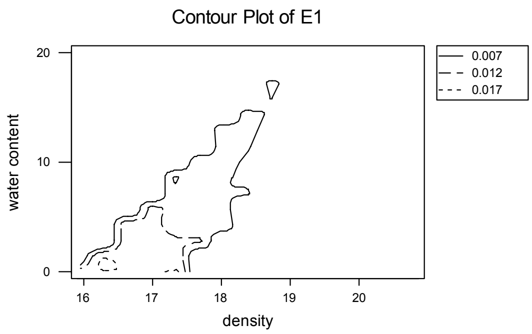

Figure 11(a): A contour representation of the variations of the first eigenvalue with water content (Wc) and density (d).

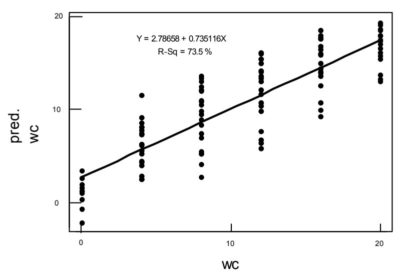

Figure 11(b): Predicted water content versus actual water content.

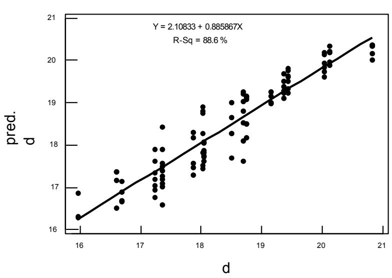

Figure 11(c): Predicted density versus actual density.

Summary and Conclusion

In this study, water contents in soils containing different fractions of bentonite with variable densities and pore fluid solute concentrations are detected using a TDR probe system and eigendecomposition technique. Samples were prepared with different combinations of bentonite fractions and moisture content and solute concentrations in soil pore fluid. Samples were compacted to various values of densities. For each experiment, reflected signals were captured by an oscilloscope and their characteristics were identified using eigendecomposition technique. Autoregressive modeling and singular value decomposition methods were utilized for calculating the eigenvalues. The most significant eigenvalues were then identified based on their power. The results indicated that the TDR probe is capable of detecting water content and clay content in tested specimens. Multivariate statistical analysis was performed and a system of nonlinear equations was developed. Actual and predicted results are in agreement, indicating a good performance and versatility of the developed system for wide range of formation water contents and densities of soil. Therefore, with the use of TDR probe and the eigendecomposition technique one could predict the water content and density of subsurface soils.

Acknowledgement

This study was supported by a research grant awarded by the Research Affairs at the UAE University.

References

[1] Topp, G.C., Davis, J.L., and Annan, A.P. (1980). Water Resources Research, 16(3):574-582.

[2] Zegelin, S.J. and White, I. (1989). Water Resources Research, Vol. 25, No. 11, pp. 2367-2376.

[3] Zegelin, S.J., White, I. and Jerkin, D.R. (1992). SSA Special Publications, Vol. 20, Madison, Wis, pp. 187-208.

[4] Young, G.D. (1996). Environmental Sensors, Inc., San Diego, CA, USA.

[5] Weitz, A.M., Grauel, W.T., Keller, M., and Veldkamp, E. (1997) Water Resources Research, 33(6):1241-1249.

[6] Yong, R.N., Mohamed, A.M.O., and Warkentin, B.P. (1992). Principles of contaminant transport in soils, Elsevier, Amsterdam, 327p.

[7] Mohamed, A.M.O., and Antia, H.E. (1998). Geoenvironmental engineering, Elsevier, Amsterdam, 707p.

[8] Marple, S. L. Jr. (1987). Digital spectral analysis with applications, Prentice-Hall, pp. 172-284.

[9] Kay, S.M. (1988). Modern spectral estimation, Prentice-Hall, pp. 153-270.

[10] Mohamed, A.M.O., Said, R.A., Al-Shawawreh, N.K., and El-Bassiouni, M.Y. (2003a). Journal of Subsurface Sensing Technologies and Applications, 4(3):159-186.

[11] Press, W.H., Teukolsky, S.A., Vetterling, W.T., and Flannery, B.P. (1992). Numerical recipes in C: The art of scientific computing, 2nd Edition, Cambridge University Press, Cambridge, 994p.

[12] Richards, W., and Seary, A. (1997). Proceedings INSNA Sunbelt XVII, San Diego, February 13-17, 1-9.

[13] Mohamed, A.M.O., Said, R.A., and El-Bassiouni, M.Y. (2003b). Environmental Geology, 45:132-143.

[14] Gould, P. (1967). Institute of British Geographers Transactions, 42:53-85.

[15] Elsner, J.B., and Tsonis, A.A. (1996). Singular spectrum analysis, Plenum Press.

[16] Said, R.A., Al-Shawawreh, N.K., Mohamed, A.M.O. (2001). Second Int. Symp. and Workshop on Time Domain Reflectometry for Innovative Geotechnical Applications, Dowding, C.H. (ed.), ©2001 by Infrastructure Technology Institute, Evanston, IL 60201, ISBN 0-9712631-0-8, 361-370.

[17] Mohamed, A.M.O., Said, R.A., and Al-Shawawreh, N.K. (2001). Second Int. Symp. and Workshop on Time Domain Reflectometry for Innovative Geotechnical Applications, Dowding, C.H. (ed.), ©2001 by Infrastructure Technology Institute, Evanston, IL 60201, ISBN 0-9712631-0-8, 371-380.

[18] Mohamed, A.M.O., Said, R.A., and Al-Shawawreh, N.K. (2002). Geotechnical Testing Journal, GTJODJ, 25(2):157-167.

[19] American Society for Testing and Materials (ASTM) (1992). Annual Book of ASTM Standards, ASTM, Philadelphia.

[20] Mohamed, A.M.O., Hawas, Y. (2004). Computer Aided Civil and Infrastructure Engineering, 19:343-356.

[21] Mohamed, A.M.O., and Said, R.A. (2004). Environmental Geology J., 47, 30-37.

[22]`Mohamed, A.M.O., and Said, R.A. (2005). Journal of Contaminant Hydrology, 76, 235-249.

[23] Sun, Z.J., Young, G.D., McFariane, R.A., and Chambers, B.M. (2000). Can. J. Soil. Sci., 80:13-22.